

COHERENT SPACE CHARGE PHENOMENA IN THE ISR

K. Hübner, E. Keil, B. Zotter
 CERN, Geneva, Switzerland.

Abstract

Coherent instabilities of bunched and coasting beams in the ISR are compared to theoretical predictions. The present phase space density is below the threshold for the longitudinal coherent instability which has not yet been observed in the ISR, while transverse instabilities have been seen and eliminated by the application of additional sextupole fields.

1. Introduction

The theory of coherent oscillations of a particle beam in a metallic vacuum chamber usually needs a number of simplifying assumptions to allow mathematical treatment. In general we have assumed cylindrical or rectangular geometry, small perturbations, and uniform particle beams. Longitudinal and transverse oscillations are treated separately, and only the dipole mode has been considered.

2. Coherent Q-shift

The betatron frequency of a transversely oscillating beam is influenced by the fields of the oscillating charges, and by the boundary conditions on the vacuum chamber and/or the magnetic pole faces. The coherent Q-shift can be expressed¹⁾ by

$$\frac{\Delta I}{\Delta Q} = - \frac{\beta \gamma Q c e}{2 r_p R^2} \left[\frac{\xi_1}{\beta^2 \gamma^2 h^2} + \epsilon_1 / h^2 + \epsilon_2 / g^2 \right]^{-1} \quad (1)$$

where the last two terms have ϵ or ξ when the magnetic field of the oscillating beam does or does not penetrate the vacuum chamber wall. For the ISR, we find for the two cases $-8,9\gamma$ A and -23γ A, where the larger figure is probably closer to reality as the thickness of the vacuum chamber is about two skindepths. Corrections for the influence of the finite conductivity of the chamber walls and for the clearing electrodes are rather small. Measurements at low current levels²⁾ gave a $\Delta I / \Delta Q$ of -7γ A. The results are shown in Fig. 1. The discrepancy between the calculated and measured values indicates that elements apart from the smooth resistive wall contribute to the Q-shift.

The incoherent $\Delta I / \Delta Q_i$ has also been measured³⁾ and was found to be about 400A at $\gamma = 16,4$, in good agreement with calculated values.

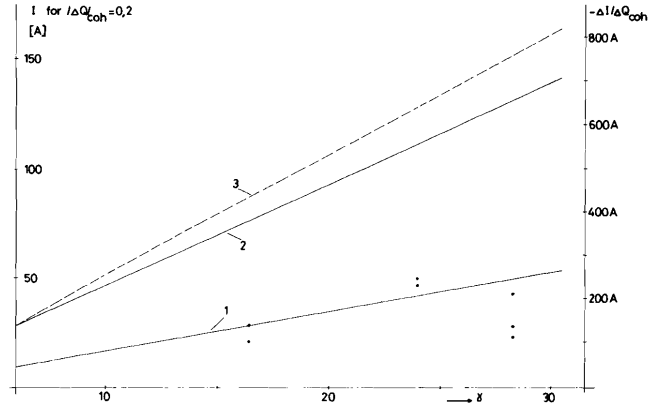


Fig.1. Current provoking a given coherent Q-shift
 Curve 1: a.c.fields penetrate vacuum chamber
 2: a.c.fields not penetrating
 3: a.c.fields not penetrating incl. finite resistivity of walls and plates.
 The dots are experimental values.

3. Coherent Transverse Instability of coasting beams

In addition to the shift of the real part of the betatron frequency, a finite wall resistivity can cause an imaginary part. This will lead to an instability of modes with $n > Q$ unless sufficient frequency spread is provided to cause Landau damping. The stability criterion can be written⁴⁾

$$\left| (n-Q) \frac{\partial \Omega}{\partial p/p} - \frac{\partial Q}{\partial p/p} \Omega \right| > \frac{1}{V'_m} \frac{V}{N} \frac{N}{\delta p/p} \quad (2)$$

where V'_m is the normalised stability limit varying between close to zero ($U > V$) and $2/\pi$ ($V \gg U$), but almost independent of the distribution function assumed. For mode numbers close to Q the Q-spread contributes most to the LHS, and we get

$$\frac{\partial Q}{\partial p/p} > \frac{1}{V'_m} \frac{V}{N} \frac{N}{\delta p/p} \quad (3)$$

For the lowest mode ($n = 9$) in a rectangular chamber corresponding to ISR dimensions we find

$$Q' \equiv \frac{\partial}{\partial p/p} > 1.3 \quad (4)$$

for a small stack ($\sim 1A$) with the actual phase space density presently obtained in the ISR. For larger stacks the criterion becomes less stringent due to the variation of the geometrical factor F_3 ⁵⁾.

In the earlier running-in tests of the ISR, sudden "brick-wall" losses were limiting the maximum intensity achievable. Application of sextupole fields to bring Q' above unity made stacking to higher intensities possible. The fact that sextupoles are an efficient cure of this transverse instability shows that it occurs at low mode numbers. It is therefore believed to be mainly due to the resistivity of the vacuum chamber. Figs.2 shows stacks ⁶⁾ made with various amounts of Q' . The beam loss at 5.5A is due to the tripping of the clearing power supplies.

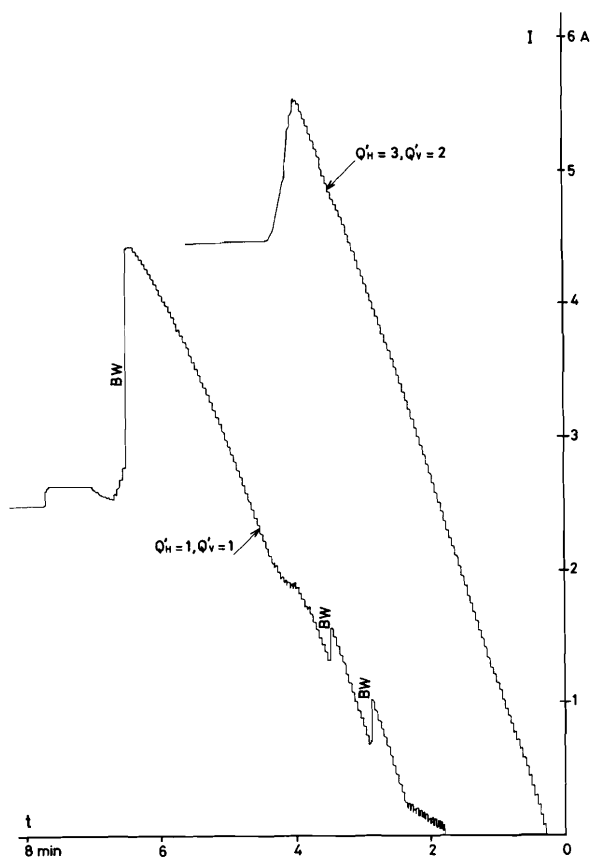


Fig. 2. Stacking with different amounts of sextupole field. The beam loss at 5.5 A is due to the tripping of the clearing power supplies.

At higher mode numbers, resonating elements of the vacuum envelope can cause large increases of V/N . An evaluation for the clearing electrodes shows, however, that the LHS of Eq. (2) increases even more due to the contribution of the spread in revolution frequency, and safety factors of over 10 are found. Also the influence of resonant cross-section variations is much smaller for the transverse than for the longitudinal case ⁷⁾.

4. Transverse bunched beam instability

Values of $Q' > 1.4$ are required to damp coherent rigid bunch oscillations, similar to the coasting beam case. However, synchrotron oscillations of the particles in the RF-bucket can provide a coupling between the front and rear end of the bunch, and lead to instable oscillation for larger values of Q' . An estimate of the growth rate due to the wall resistivity (without Landau damping) is given by ^{8,9)}

$$\beta_m = -0.466 \frac{r_p c}{b^3 \mu^{1/2} \delta^{1/2}} \frac{N}{2\gamma \omega_{QA}^{1/2}} C_m \times G_m(\chi) \quad (5)$$

where

$$\chi = - \frac{2A\omega_n Q'}{Q} \quad (6)$$

is the phase shift between front and rear end of the bunch. For typical ISR parameters, $\chi = 4.6 Q'$ and only higher modes ($m > 2$) should be unstable for a positive Q' . As the maximum growth rate is only 2 sec^{-1} , Landau damping should be effective. For a negative Q' also the lowest mode ($m = 0$) can become instable with a growth rate of about 13 sec^{-1} .

Transverse instability at injection has been seen in the ISR, and the beam blows up horizontally. $Q' > 1$ suppresses the instability, while $Q' = -2$ does not. The growth-rate does not vanish for small Q' , but is of order of 100 sec^{-1} contrary to the head-tail effect theory.

5. Evolution of the Mode Spectrum

A large number of signals have been seen on a spectrum analyser with a frequency response from 0 - 110 MHz connected to pick-up plates, both during injection and with a circulating beam. During injection, sidebands of the multiples of the revolution frequency are usually seen at $(n-Q)$, but also at other frequencies corresponding to $(Q-n)$ and $(n-2Q)$ modes.

With circulating beams of a few amperes, single lines or clusters of lines corresponding to $(n-Q)$ modes have been observed between 30 and 70 MHz, and sometimes as high as the upper frequency limit of the analyser. Some lines appear stationary, remaining for minutes, other drift downwards in frequency, covering as much as 10 MHz in a few minutes. There are no obvious resonant elements at those frequencies; this explanation would not fit the drifting lines in any case. One tentative explanation which has been proposed is by electrons oscillating in the potential well of the proton beam ¹⁰⁾, which may render transverse proton beam

modes unstable. Their frequency would lie roughly in the observed range.

$$\omega_{el}^2 = \frac{2Nc^2 r_e}{\pi Rb(b+a)} \approx 100 \text{ MHz} \quad (7)$$

Fig. 3 shows a typical spectrum analyser output.

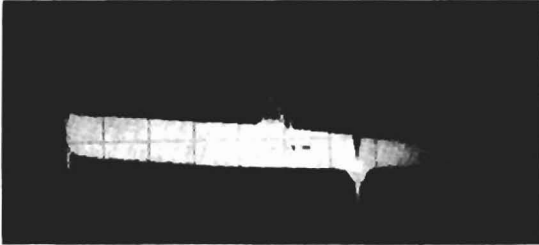


Fig. 3. Frequency spectrum extending from 0-100MHz picked up by a plate at a current level of 3,5A. The negative spike is instrumental.

6. Coherent longitudinal instabilities

The criterion for stability of coherent longitudinal oscillations of the beam can be written¹¹⁾

$$|Z/n| < (E_0 n / e \gamma I_0) (\Delta p / m_0 c)^2 \quad (8)$$

where Z/n is the coupling impedance divided by the mode number. For the first few injected pulses, the limit on Z/n at design phase space density is of the order of 10Ω , and much larger ($\sim 1k\Omega$) for a full stack with not too steep flanks. Because the design density has not yet been obtained, the present limit should be about 100Ω .

At the lowest mode ($n = 1$) the resistive wall contributes about 5Ω , while most other equipment (clearing electrodes, guard plates of pick-up stations, inflection kicker screen, cross-section variations, RF cavities) contribute inductively of the order of 10 to 20 $i \Omega$. For increasing mode numbers, the resistive wall contribution decreases as n^{-2} . At the resonant frequency of the RF cavities, the coupling impedance has been reduced to a few Ω by feedback.

At even higher frequencies, many different elements of the vacuum envelope become resonant. The coupling impedance then equals roughly the product of the low frequency value and the quality factor. For example, the large number (~ 300) of variations from elliptical to circular cross-section have been calculated to contribute about 3.5Ω per pair, yielding close to $1k\Omega$ if they all add in phase. Large tanks can yield even higher impedances given roughly by¹²⁾.

$$\left(\frac{Z}{n}\right)_{res} = 200 \frac{\beta^3 \sigma^4 l^2}{Rg} (2d)^{\frac{5}{2}} \phi \left(\frac{b}{d}\right) \sin^2 \left[2.4 \frac{R}{2d} X \left(\frac{b}{d}\right) \right] \quad (9)$$

where ϕ lies between zero and one and expresses the correction due to the side-hole, and $X > 1$ the frequency correction. A more detailed analysis, taking the finite resistivity of the side tubes into account, uses matrices evaluated numerically by computer¹³⁾.

Measurements of the frequency response of various elements have shown high Q -resonances¹⁴⁾ in the lower microwave region, but no unambiguous microwave signals have been picked up from the beam.

7. Conclusions

The agreement of theory and experiment of the transverse resistive wall instability is quite satisfactory, and the application of the calculated amount of sextupole component led to its disappearance. The situation is less clear for the longitudinal case, where theory predicts too large coupling impedances in the microwave region due to resonant elements, but no direct evidence for an instability has been obtained so far. At present, the beam intensity does not seem to be limited by coherent effects.

References

- 1) L.J. Laslett, L. Resegotti; 6th Int. Conf. on High Energy Acc., 1967, p.150
- 2) K. Hübner; ISR Running-in report (Run 89) 26.7.1971 (unpublished)
ISR Running-in report (Run 105, 107, 110), 14.9.1971 (unpublished)
- 3) J.P. Gourber and H. Laeger; ISR Running-in report (Run 105), 8.9.1971 (unpublished)
- 4) K. Hübner, P. Strolin, V. Vaccaro, B. Zotter ; CERN/ISR-RF-TH/70-2
- 5) B. Zotter ; CERN/ISR-TH/68-51
- 6) B. Zotter ; ISR Running-in report (Run 84), 12.7.1971 (unpublished)
- 7) W. Schnell ; CERN/ISR-RF/70-7
B. Zotter ; CERN/ISR-TH/71-13
- 8) K. Hübner, B. Zotter ; CERN/ISR-TH/71-18
- 9) M. Sands ; SLAC-TN-69/8 and 10
B. Zotter; CERN/ISR-TH/69-60
- 10) H.G. Hereward ; CERN-71, to be published
- 11) E. Keil, W. Schnell; CERN/ISR-RF-TH/69-48
- 12) E. Keil, B. Zotter ; CERN/ISR-TH/70-30 and 33
B. Zotter ; CERN/ISR-TH/70-47
- 13) E. Keil, B. Zotter ; Particle Accelerators (to be published)
- 14) P. Bramham ; BEIC document No. 64, 5.7.1971 (unpublished)